

N74 30944

**FACTORS AFFECTING THE STRENGTH OF
MULTIPASS LOW-ALLOY STEEL WELD METAL**

By

Boris M. Krantz

**MANAGER, METALLURGICAL DEVELOPMENT
FILLER METALS RESEARCH AND DEVELOPMENT DEPARTMENT
AIRCO WELDING PRODUCTS
MURRAY HILL, NEW JERSEY**

465<

ABSTRACT

The mechanical properties of multipass high-strength steel weld metals depend upon several factors, among the most important being 1) the interaction between the alloy composition and weld metal cooling rate which determines the as-deposited micro-structure, and 2) the thermal effects of subsequent passes on each underlying pass which alter the original microstructure. The bulk properties of a multipass weld are therefore governed by both the initial microstructure of each weld pass and its subsequent thermal history. Data obtained for a high-strength low-alloy steel weld metal have confirmed that a simple correlation exists between mechanical properties and welding conditions if the latter are in turn correlated as weld cooling rate.

This report summarizes the results of both metallographic analysis and tensile tests of weld metal synthetically subjected to the thermal history occurring in 2-in. GMA weldments made at both the lower- and upper-limit of the practical range of energy input-plate temperature conditions. The yield strength of the weld metal deposited at 40 kJ/in-200°F and after subsequent austenitizing is approximately 175 ksi. Further exposure of this fully martensitic weld metal to peak temperatures in the inter-critical range formed significant amounts of ferrite which reduced the yield strength to 140 ksi. Further thermal treatments at several sub-critical tempering temperatures produced marked carbide spheroidization and agglomeration but no change in yield strength. The resultant final microstructure was therefore a mixture of ferrite and tempered martensite having a yield strength of approximately 140 ksi.

The weld metal deposited at 60 kj/in-300°F was cooled at rates slow enough to cause transformation to proeutectoid ferrite and possibly upper bainite, the combination of which produced a yield strength of 152 ksi. Reaustenitizing this as-deposited structure lowers the yield strength to 144 ksi due to the additional formation of ferrite and bainite. Subsequent cycling within the intercritical region produced more ferrite and a decrease in yield strength to 137 ksi. The structure of multipass AX-140 weld metal deposited at 60 kj/in-300°F is thus comprised of tempered martensite, ferrite and tempered bainite, the latter two constituents accounting for the lower strength of weld metal deposited at relatively high energy inputs.

INTRODUCTION

The mechanical properties of high-strength low-alloy steel weld metals are influenced by many factors. Probably the most significant factors with alloys designed to produce yield strengths in the range of 100-150 ksi are the composition, the solidification substructure, and the solid state transformations occurring during both the initial cooling and the multiple thermal cycles resulting from subsequent passes in a multipass weld. Although the importance of the first two parameters cannot be ignored, the latter two are of special interest since they can be controlled readily by proper selection of welding parameters. Several studies (1,2) have shown that the yield strengths of such weld metals are decreased markedly when relatively high levels of welding energy-input and/or plate preheat temperature are used. As a result of these investigations, recommended ranges of welding conditions have been specified for each composition of weld metal in order to achieve satisfactory mechanical properties.

An analysis of data generated in a series of AX-140 welds has shown that a simple correlation exists between weld-metal strength and welding conditions if these conditions are expressed as the corresponding weld cooling rates (1). When interpreted in this fashion, it is clear that rapid losses in strength occur when the weld metal is deposited with conditions causing cooling rates slower than a certain critical level. The mechanism

commonly postulated to explain this pronounced softening has been the formation of non-martensitic microconstituents. Knowledge of the continuous-cooling transformation characteristics have thus enabled the minimum-allowable cooling rate to be defined. This, in turn, allows one to define the combination of welding energy input and preheat temperature for a given plate thickness to avoid the formation of a weak phase during the initial cooling of each weld pass. However, this information is incomplete since every pass in a multipass weldment is "heat-treated" by the thermal cycles caused by subsequently-deposited passes. Thus the resultant mechanical properties of a multipass weld must be governed as much by the microstructural changes produced by repetitive thermal treatments of the initially-deposited structures as they are by the characteristics of the initial structure. The real question to be answered is whether the strength-limiting factor is predominantly the initially-formed structure or the heat-treating effect of subsequent thermal cycles.

The purposes of this program have been (a) to determine the microstructures of as-deposited GMA weld metal made at typical low- and high-energy inputs and to define their effect on mechanical properties, and (b) to determine the changes occurring in these microstructures and the final mechanical properties as a result of the thermal cycling in multipass weldments. The latter effects were studied with miniature weld metal specimens each of which contained only that microstructure characterizing a particular set of weld thermal cycles, and which were used to

determine the sequential changes in the properties of a specific region of a multipass weld metal.

EXPERIMENTAL PROCEDURE

Experiments were designed to reproduce synthetically the metallurgical and mechanical property changes occurring in as-deposited weld metal as the result of multipass welding. Microstructural changes were studied using conventional optical and electron microscopy techniques. Tensile properties were determined using miniature tensile specimens initially machined from actual weld passes deposited at specific welding conditions (see Table 1) and then subjected to thermal cycles typical of 2-in. thick multipass welds. To insure an essentially identical composition in all specimens, they were taken from an AX-140 weld pad as shown in Fig. 1, to avoid dilution with the base plate. Table 2 shows the chemical analysis of both sets of specimens and confirms that identical analyses were obtained. The AX-140 weld pad was deposited on 2-in. thick HY-130(T) plate to insure that heavy plate cooling conditions existed. The weld deposits were spaced sufficiently far apart to insure that the thermal effects caused by one weld deposit would not affect those already made. To insure that the specimens consisted entirely of as-deposited beads, transverse sections of the rough-machined blanks were ground and etched to locate the specimen center for final machining.

The finish-machined specimens were heat-treated in the Duffers' Gleeble (3) and subjected to the thermal cycles recorded when depositing multipass welds at 40 kj/in-200°F and 60 kj/in-300°F. The specific sets of peak temperatures to which the specimens were exposed are presented below:

PEAK TEMPERATURE OF THERMAL CYCLES PRODUCED
WITHIN A TYPICAL PASS DURING MULTIPASS WELDING

<u>Energy Input</u>	<u>Preheat Temperature</u>	<u>Peak Temperature °F</u>
40 kj/in.	200°F	1890 - 1365 - 895 - 415 - 380
60 kj/in.	300°F	1900 - 1400 - 995 - 975 - 780 - 770

It should be noted that although thermal cycles having similar peak temperatures were observed at each set of welding conditions, the measured cooling rates are significantly slower at the 60 kj/in-300°F conditions. Therefore, significantly different microstructures were produced, as will be described in a following section of this paper. The heat-treated specimens were machined to the miniature tensile specimen configuration shown in Fig. 1. The reduced section, 0.092-in. length and 0.045-in.dia., was machined so that the prior position of the control thermocouple (percussion-welded on the specimen during Gleeble heat treatment) was centered within the reduced gage length. Tensile tests were made with a standard Instron testing machine at a cross-heat travel speed of 0.02-in/min.

The tensile strengths reported were calculated from the maximum sustained load and the initial sample cross-section area. The reported 0.2% offset yield strengths were estimated from the load-crosshead extension data by assuming that the crosshead travel causes uniform strain only within the reduced gage length. Analyses of the experimental errors in load measurement and of

one standard deviation in measuring cross-section area indicated a maximum error of $\pm 3\%$ in the resulting tensile strength data.

Prior metallographic studies and mechanical tests of thermally-cycled specimens showed that significant decreases in strength should be expected when the as-deposited welds are reheat-treated. This softening could not be explained by the formation of bainite rather than martensite as indicated by the accepted continuous cooling diagram for AX-140. Accordingly, the transformation characteristics were rechecked with the rapid response, high-resolution dilatometer of the Duffers' Gleeble. The net resolution of this system in combination with the instrumentation of temperature and specimen dilation permitted volume changes of 0.05% to be detected in the 0.250-in.diam. specimens used. Additional evidence of transformation was also obtained by the inverse cooling rate method described in a subsequent section of this paper.

RESULTS AND DISCUSSION

CONTINUOUS-COOLING DIAGRAM FOR AX-140 WELD METAL

The AX-140 continuous cooling transformation diagram obtained in this investigation is shown in Fig. 2. The significant difference in comparison to the previously-accepted diagram is the addition of a ferrite-start (Fs) transformation line. The remainder of the diagram, i.e., the occurrence of a martensite-start (Ms) line at 780°F and an upper bainite-start (Bs) line, is essentially identical to the published CCT diagram. Superimposed on this figure are bands of initial cooling cycles measured at 40 kJ/in.-200°F and 60 kJ/in.-300°F welding conditions. According to these data, a martensitic microstructure will form during cooling to room temperature when AX-140 weld metal is cooled at rates equal to or faster than those characterizing the 40 kJ/in.-200°F welding conditions. However, when this weld metal is deposited at the slower-cooling rates characterizing the 60 kJ/in.-300°F welding conditions, the diagram predicts the formation of proeutectoid ferrite prior to the martensite transformation assumed to predominate. Upper bainite is an additional transformation product probably formed during these cooling conditions. The net result at room temperature is a mixture of ferrite and upper bainite in a predominantly-martensitic matrix. The influence of these cooling conditions upon the weld metal

morphology and tensile properties was revealed by conventional replica electron microscopy and mechanical tests of heat-treated weld metals.

METALLOGRAPHIC AND MECHANICAL PROPERTIES OF AS-DEPOSITED AND THERMALLY-CYCLED WELD METALS

The tensile and yield strengths of the as-deposited and thermally-cycled welds are plotted in Fig. 3 as a function of their cumulative thermal history shown schematically at the bottom of the figure. Both the metallographic observations and the strength measurements of each weld metal were made in the as-deposited condition, again after the as-deposited specimens were reaustenitized by a weld thermal cycle having a peak temperature of 1900°F, and after each of the subsequent weld thermal cycles. The data thus indicate the sequential changes in microstructure and mechanical properties occurring in typical underlying passes in 2-in. multipass weldments made at both 40 kj/in.-200°F and 60 kj/in.-300°F welding conditions.

Influence of 40 kj/in. Energy Input and 200°F Preheat Temperature

As shown at the left of Fig. 3, the tensile and yield strengths of weld metal deposited at 40 kj/in.-200°F are 182 and 177 ksi, respectively. Similar strengths were observed after the sample was reaustenitized at 1890°F. Examination of

the CCT diagram in Fig. 2 indicates that a fully martensitic microstructure is produced during the initial cooling cycle from the fused state. The sample heated to an 1890⁰ peak temperature cools at virtually the identical rate. The conclusion is logically drawn that both the initial as-deposited and the reaustenitized weld metals are completely martensitic, and that the strengths in both conditions should be similar. The high strength levels observed also serve as indirect proof that martensite is present since the tensile strength of a 0.1%C steel fully quenched to martensite is reported to be approximately 180 ksi (4). Electron micrographs of replicas at magnifications of 3000X (Figs. 4 and 5) show the 40 kj/in. weld metal specimens in both the as-deposited and as-deposited plus 1890⁰F reaustenitized conditions to have an extremely fine acicular morphology arrayed in the pseudo- (111) geometry indicative of the low-carbon martensite (5).

The presence of a completely martensitic structure after both the as-deposited cooling cycle and the 1890⁰F peak temperature thermal cycle also is evident in Fig. 6a, an inverse cooling rate plot of the cooling cycle of the 1890⁰F thermal cycle. This classic technique (6) enables the detection of exothermic phase changes otherwise undetectable by observation of conventional cooling curves. The 1100⁰ - 800⁰F range of temperature experiences a continuous decrease in cooling rate shown by a gradual increase in the length of time to cool a fixed number of degrees. The marked change occurring between 800 and 780⁰ indicates the occurrence

of an exothermic phase transformation, this being the formation of martensite. The further perturbation at 740°F is probably due to the continued formation of martensite and not to any new phase formation. Therefore, the as-deposited cooling cycles must behave similarly to the austenitizing cycle just described since their cooling rates are essentially identical.

Exposure of the reaustenitized weld metal to a weld thermal cycle with a peak temperature of 1365°F results in large decreases in both the tensile and yield strength to levels of 156 and 138 ksi, respectively. This is due to the formation of ferrite during the partially austenitizing heat treatment, a phenomenon also reported (7) to occur in low-carbon low-alloy steel weld heat-affected zones. The ferrite formed during the intercritical thermal cycle appears as relatively large, featureless microconstituents shown in Figs. 7a and 7b, electron micrographs taken at magnifications of 3000X and 5500X, respectively. Note that the overall acicularity is retained and that the prior structure (shown in Fig. 5) displayed none of these constituents believed to be ferrite. A lineal analysis of the area fraction of ferrite indicated this phase to comprise approximately 55% of the microstructure. This amount is much lower than the 75 - 80% predicted from the conventional Fe-C metastable phase diagram. But when the eutectoid composition and the A_1 - and A_3 -phase boundaries are modified (8) for the AX-140 composition, the presence of ferrite in these quantities can be predicted by conventional lever-law calculations.

Figs. 8a and 8b are electron micrographs taken at magnifications of 5375X and 12,000X, respectively, after the partially-ferritic weld metal was exposed to an additional weld thermal cycle with a peak temperature of 895°F. Clearly visible in both these micrographs is the tempering effect of the 895°F peak temperature thermal cycle and the resultant precipitation of carbides. Similar structures were observed in specimens subsequently subjected to the 415 and 380°F peak temperature thermal cycles. Tempering of the martensite and aging of the super-saturated ferrite formed during the rapid intercritical treatment are the principal phenomena occurring in this series of specimens, i.e., the 895, 415, and 380°F peak temperature thermal cycles. The tensile and yield strengths observed showed some variability, however, no significant decreases were observed.

Influence of 60 kj/in-300°F Weld Thermal Cycles

The mechanical properties of various regions of multipass welds made at 60 kj/in. with 300°F preheat are also shown in Fig. 3. These are significantly weaker than equivalent AX-140 welds deposited at 40 kj/in. and 200°F. The as-deposited tensile and yield strengths are 169- and 152-ksi for the 60 kj/in-200°F weld metal as compared to 182- and 177-ksi for the faster-cooled 40 kj/in-300°F weldment. Based upon the continuous-cooling diagram, the decrease in strength in the 60 kj/in-300°F is due to the formation of ferrite at 950 - 1000°F, upper bainite at 800°F, and martensite at 780°F. Thus, the final room temperature

microstructure is comprised of ferrite, upper bainite and martensite. This microstructure is shown in Figs. 9a and 9b. Both of these electron micrographs were taken at magnifications of 5500X and 12,000X, respectively. The relative proportion of these phases was not determined due to the extensive and difficult metallographic effort required. However, it seems reasonable to assume the presence of more martensite than bainite in these structures since the diffusion-controlled bainite transformation occurs for only 2 to 3 seconds prior to the beginning of the martensite transformation. Thus it is unlikely that any large amounts of upper bainite could form.

Reaustenitizing the as-deposited microstructure at 1900°F significantly decreased the tensile- and yield-strength to 159- and 144-ksi, respectively. The cooling cycle from the 1900°F peak temperature is slower than the initial cooling, thus permitting longer times to form both ferrite and bainite. Therefore, when compared to the as-deposited microstructure, it is reasonable to assume a larger volume fraction of ferrite and bainite in the overall structure, and, thus a lower strength. Typical electron micrographs of this structure are shown in Figs. 10a and 10b at magnifications of 5500 and 13,000X, respectively. Somewhat coarser, but nevertheless similar features to those of the as-deposited structure are visible in both micrographs since no major differences in structure would be predicted from the weld metal's transformation characteristics. The presence of ferrite also was independently confirmed with the inverse-cooling-rate analysis of the 1900°F peak temperature thermal cycle as

shown in Fig. 6b. More scatter is evident than in the 40 kj/in-200°F curve, but a major transformation is clearly apparent at approximately 950°F as is the martensite formation at approximately 780°F. These data verify the ferrite formation detected by means of dilatometry.

The sample treated at 1900°F was partially reaustenitized with an additional weld thermal cycle having a peak temperature of 1400°F. This resulted in a continued loss in both tensile and yield strength to levels of 145- and 132-ksi, respectively. As was the case with the 40 kj/in-200°F weld metal, the resulting microstructure consisted of a partially-transformed ferrite-bainite and/or martensite aggregate as shown in Figs. 11a and 11b. Clearly evident in these electromicrographs are ferritic-microconstituents dispersed in a bainite-martensite matrix. The area fraction ferrite was approximately 63% compared to the 72% level predicted on the basis of a modified equilibrium diagram.

Continued exposure of the mixed ferrite-bainite microstructure to three more weld thermal cycles having peak temperatures of 995, 780 and 770°F caused no significant change in tensile and yield strengths, the final levels being 146- and 132-ksi, respectively. The microstructures produced after each of these heat treatments show the anticipated precipitation of carbides resulting from the combined effects of tempering the martensite and/or bainite and aging the supersaturated ferrite. Typical microstructures are shown in Figs. 12a and 12b, electron

micrographs taken at magnifications of 5375X and 12,000X, respectively. Again, in similar fashion to the behavior observed after tempering the lower energy-input weld metals, clear evidence of precipitation is present within both microconstituents, although no change in tensile properties occurs. The resultant microstructure is, therefore, comprised of a mixture of tempered martensite and bainite together with aged ferrite.

Summary of Weld Metal Reheat-Treatment Studies

The results of mechanical tests of both series of weld metals indicate the marked influence of both the initial weld cooling rates and the subsequent heating cycles which affect the formation of ferrite in the microstructure and properties of individual weld deposits. These data have shown that AX-140, and by inference, any metallurgically-similar high-strength low-alloy steel weld metal when initially deposited at cooling rates sufficiently fast to form martensite possesses a very high strength and is weakened significantly after exposure to a series of weld thermal cycles having peak temperatures between the upper and lower critical temperatures.

Confirmation that conventionally-measured tensile properties of multipass welds are controlled by thermal effects as described in the results of this study is shown in Table 3. These data compare typical ultimate tensile strengths of multipass 2-in. GMA weldments (9) with those of the miniature weld metal specimens subjected to the entire series of weld thermal cycles. Although

the data for the multipass and thermally-cycled specimens differ by approximately 6%, a discrepancy of this magnitude is considered small considering the type of comparison being made. It was concluded that the approach used in this investigation to synthesize the microstructural and mechanical property changes occurring in underlying passes was valid and represents with good accuracy the phenomena occurring within an actual weldment. Since the multiplicity of thermal cycles cannot be avoided in a multipass weldment with the ensuing formation of ferrite, the only strength-limiting factor left to the control of the welding engineer or metallurgist is the formation of proeutectoid ferrite during initial cooling of each weld pass, i.e., by maintaining a maximum practical weld cooling rate. In the AX-140 system, or in any other high-strength low-alloy steel weld metal, this is accomplished by specifying maximum levels of both energy input and plate temperature, the adherence to which will insure minimum weld metal strength levels.

ACKNOWLEDGEMENT

now of Electrotherm Corp.

The author wishes to acknowledge with thanks, K. Dorsch^A and A. Lesnewich of Airco for the contribution of their experience gained in the initial studies of process effects on weld metal properties and J. Devine for performing with precision and accuracy the dilatometry studies which provided key technical information in this investigation. In addition, appreciation must also go to the Naval Ship Systems Command of the U.S. Navy for its sponsorship under Contract NObS - 94535 (FBM).

REFERENCES

- (1) DORSCHU, K.E.
Control of Cooling Rates in Steel Weld Metal.
Welding Journal, 48(2) (1969).
- (2) CONNOR, L.P. et al
Development of Procedures for Welding HY-130(T) Steel.
Welding Journal, 46(7): 309s - 321s (1967).
- (3) NIPPES, E.F. and SAVAGE, W.F.
Development of Specimen Simulating Weld Heat-Affected-Zones
Welding Journal, 28(11): 534s - 546s (1949).
- (4) BAIN, E.C. and PAXTON, H.W.
Alloying Elements in Steel.
ASM, Metals Park, Ohio (1966).
- (5) WAYMAN, C.M.
Introduction to the Crystallography of Martensitic Transformations.
N.Y. MacMillan Company, 1964.
- (6) KEHL, G.L.
Principles of Metallographic Laboratory Practice.
N.Y., McGraw Hill, 1949.
- (7) SAVAGE, W.F. and OWCZARSKI, W.A.
The Microstructure and Notch Impact Behavior of a Welded Structural Steel.
Welding Journal, 45(2): 55s - 65s (1966).
- (8) ANDREWS, K.W.
Empirical Formulae for the Calculation of Some Transformation Temperatures.
JISI, July 1965. pp. 721 - 727.
- (9) DORSCHU, K.E.
HY-130/150 weldments: Summary report on the development of filler metals and joining procedures.
Air Reduction Co, Inc., Murray Hill, N.J.
Report to Bureau of Ships, Contract No. NObs 88540, SR007-01-01, Task 853.
RE-66-014-CRE-34 (January 26, 1966).

TABLE 1

**GAS-METAL-ARC WELDING CONDITIONS FOR 2-IN.
THICK HY-130(T) WELDMENTS**

Airco Weld No.	2444-17	2444-25
• Energy input (kj/in.)	40	60
Preheat/interpass (°F)	200/225	300/325
Current (amp)	270	285
Voltage (DCRP)	25	25
Travel Speed (ipm)	10	7
Electrode Extension (in.)	3/4	3/4
Shield Gas	A-2% O ₂ at 50 cfh	A-2% O ₂ at 50 cfh
Wire Diameter (in.)*	1/16	1/16
Wire Feed Speed (ipm)	140	195

*Wire from heat 1P0047 of AX-140 welding wire.

TABLE 2

CHEMICAL ANALYSIS OF HEAT-TREATED AX-140
GMA WELD METAL SPECIMENS

	40 kj/in-200°F Welding Conditions	60 kj/in-300°F Welding Conditions
C	0.092	0.090
P	0.008	0.007
S	0.007	0.007
Si	0.24	0.22
Mn	1.62	1.58
Ni	2.25	2.24
Cr	0.88	0.87
Mo	0.57	0.56
W	0.017	0.013
Nb	0.004	0.004
V	0.013	0.013
Cu	0.088	0.088
Co	0.017	0.015
Al	0.009	0.005
Zr	--	--
Ti	0.008	0.006
B	0.0007	0.0008
Sn	0.011	0.011

Note: Above analyses obtained by vacuum spectrographic analysis of samples of chips from each weld metal.

C-6

TABLE 3

COMPARATIVE ULTIMATE TENSILE STRENGTHS OF CONVENTIONAL
AND THERMALLY-CYCLED WELD METAL TENSILE SPECIMENS

	Ultimate Tensile Strength (ksi)	
	40 KJ/IN-200 ⁰ F	60 KJ/IN-300 ⁰ F
Conventional Bulk Weld Metal Specimens	159	157
Thermally-cycled Specimens	150	144

13 pieces

31-0

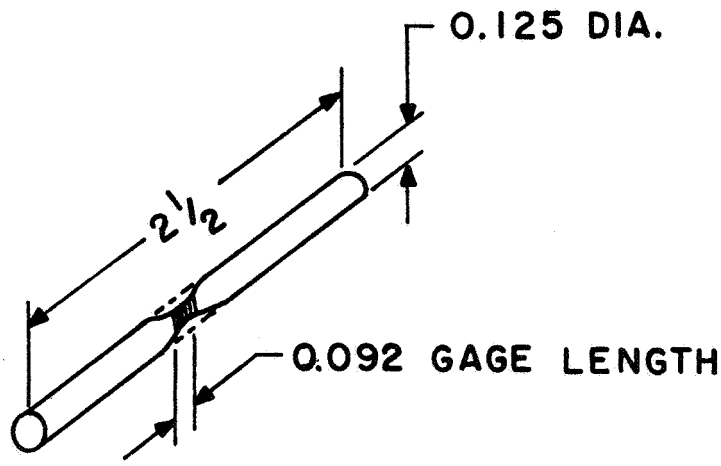
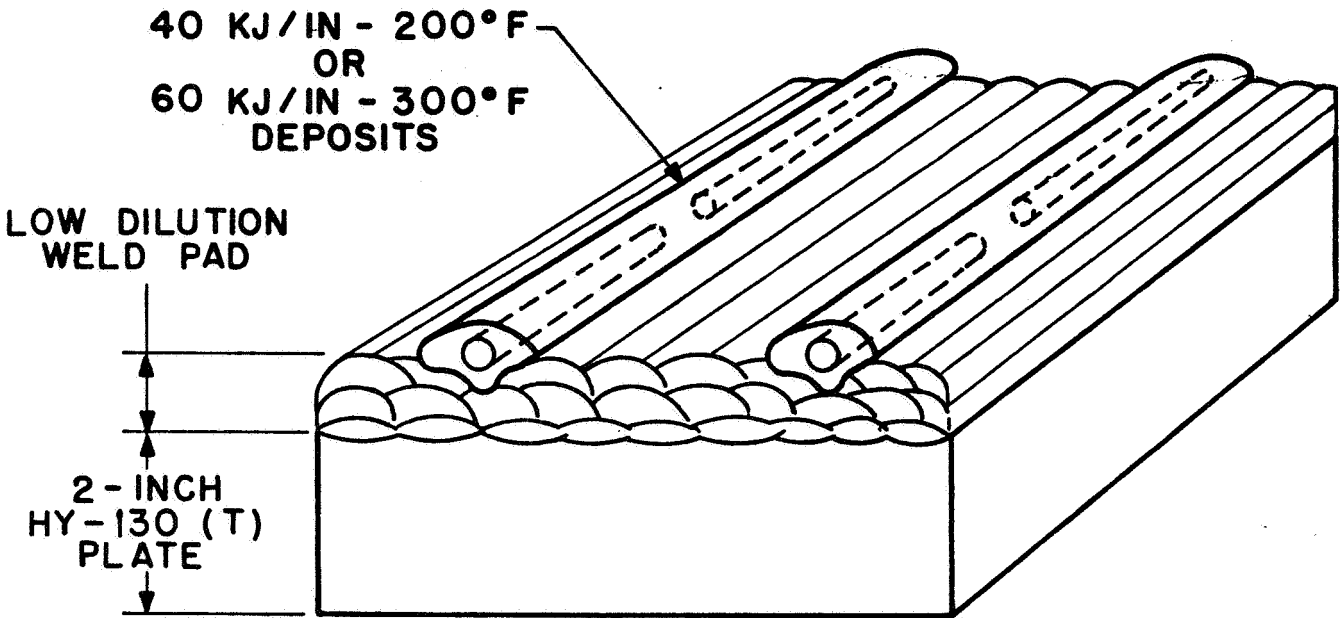
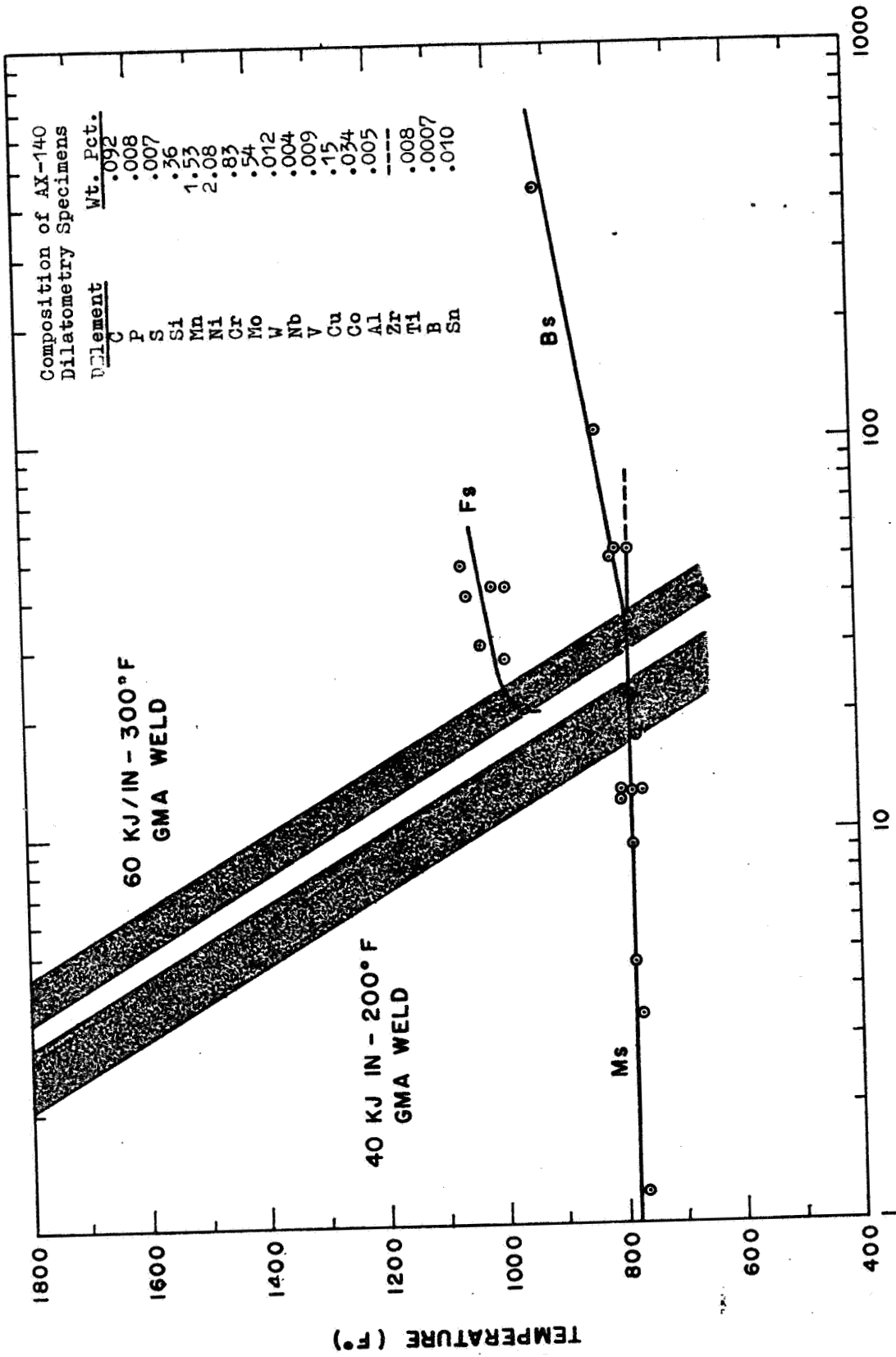


Figure 1. - Schematic representation of specimen preparation.

40 p. at



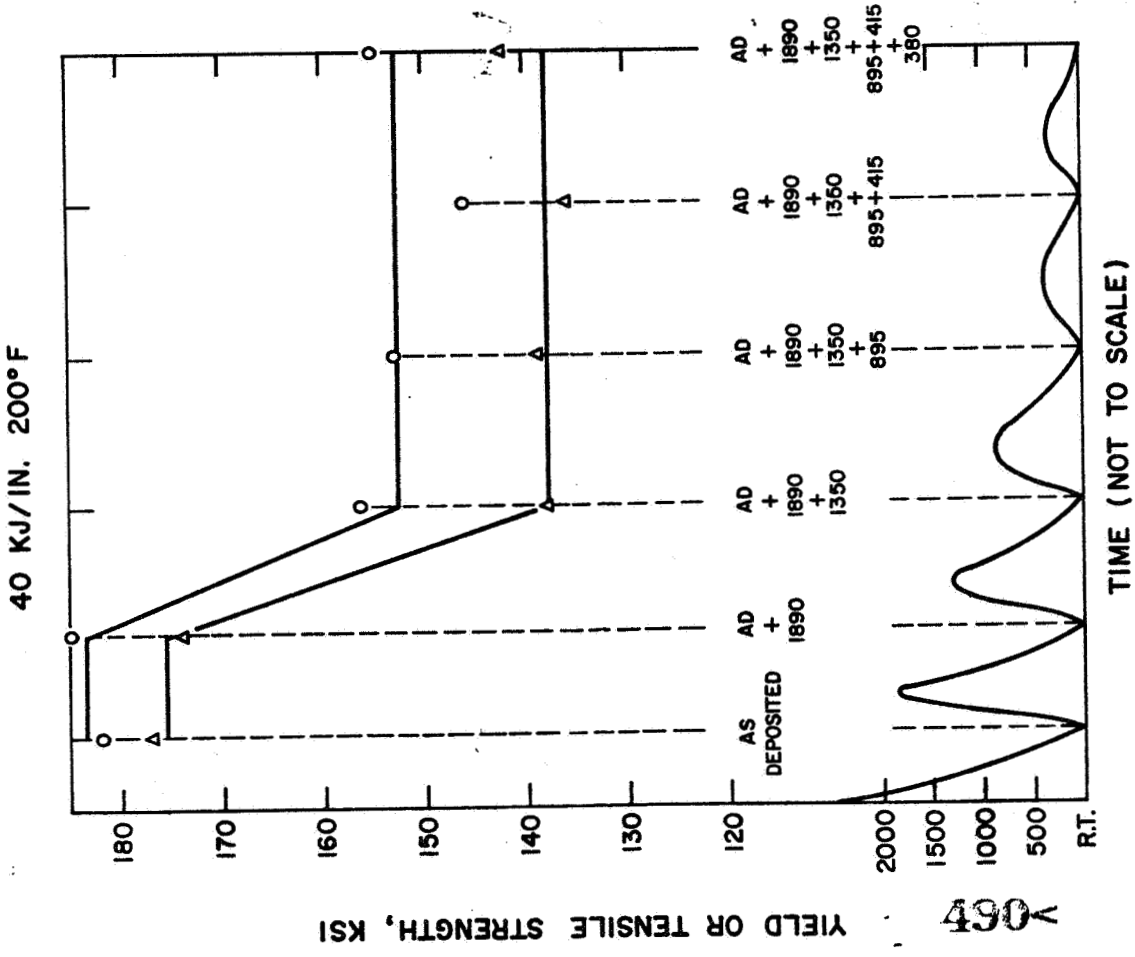
489<

Figure 2

Fig 2 - Kientz

GAS METAL ARC WELDING CONDITIONS

40 KJ/IN. 200°F



60 KJ/IN. 300°F

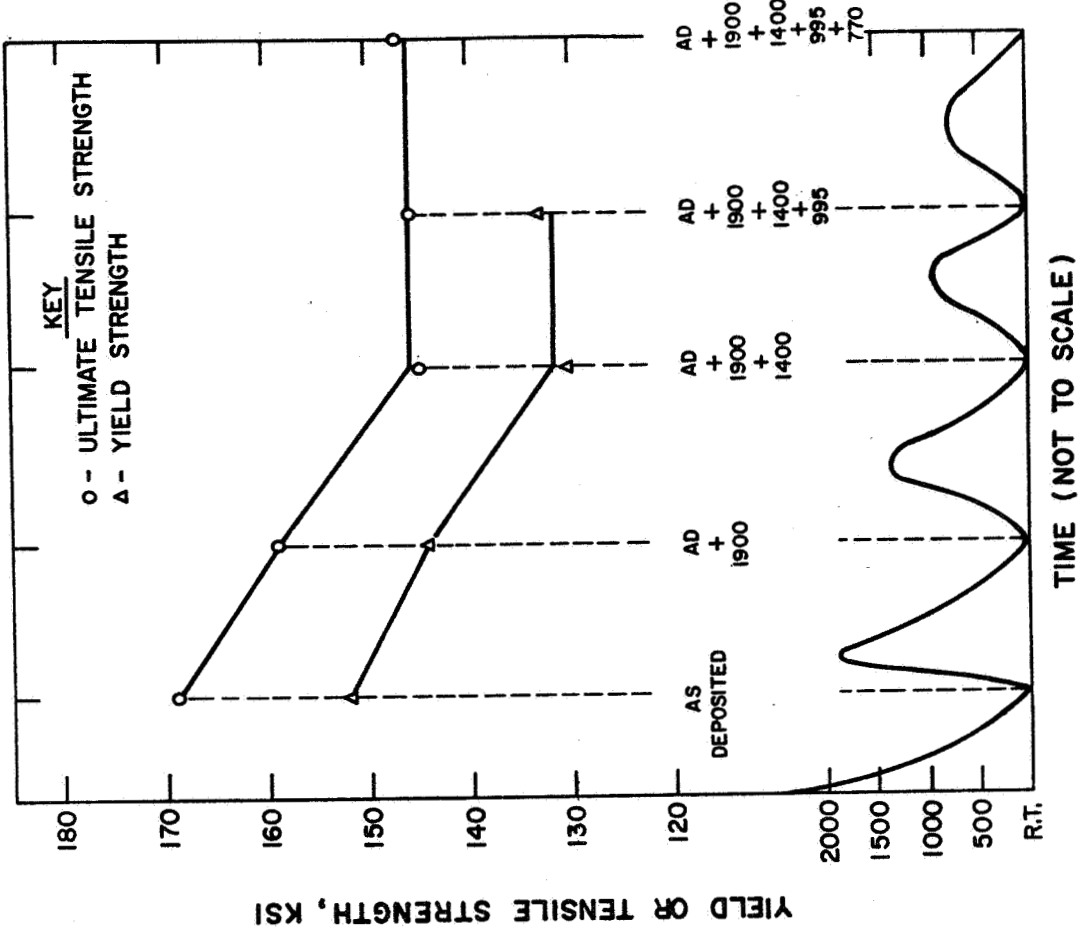


Figure 3

Fig 3 - Krantz

67.5

~~67.5~~

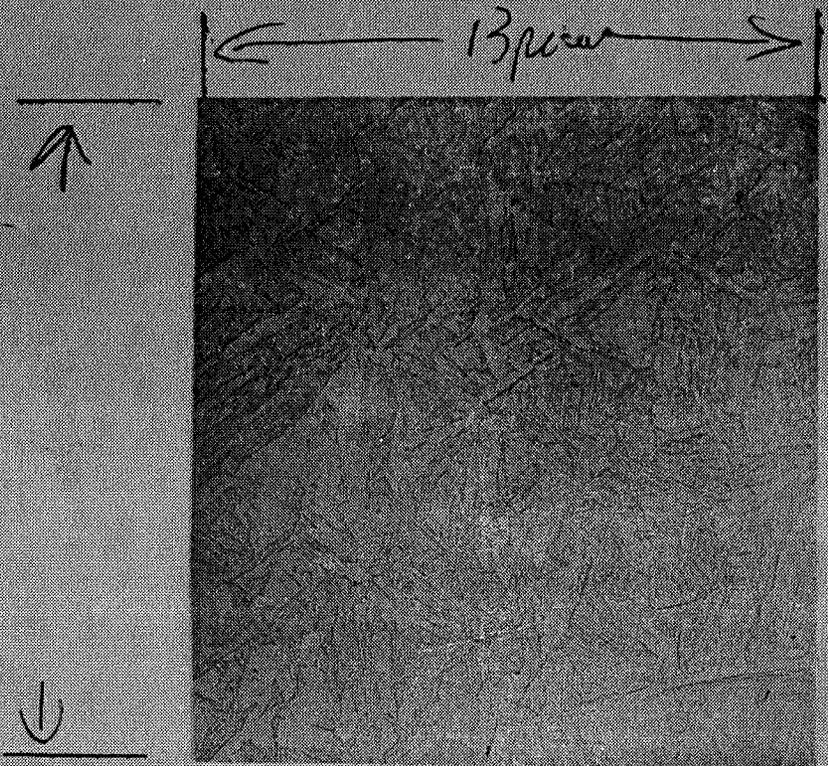


Figure 4

63.8

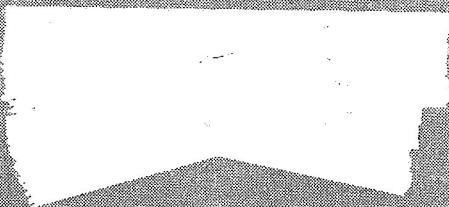
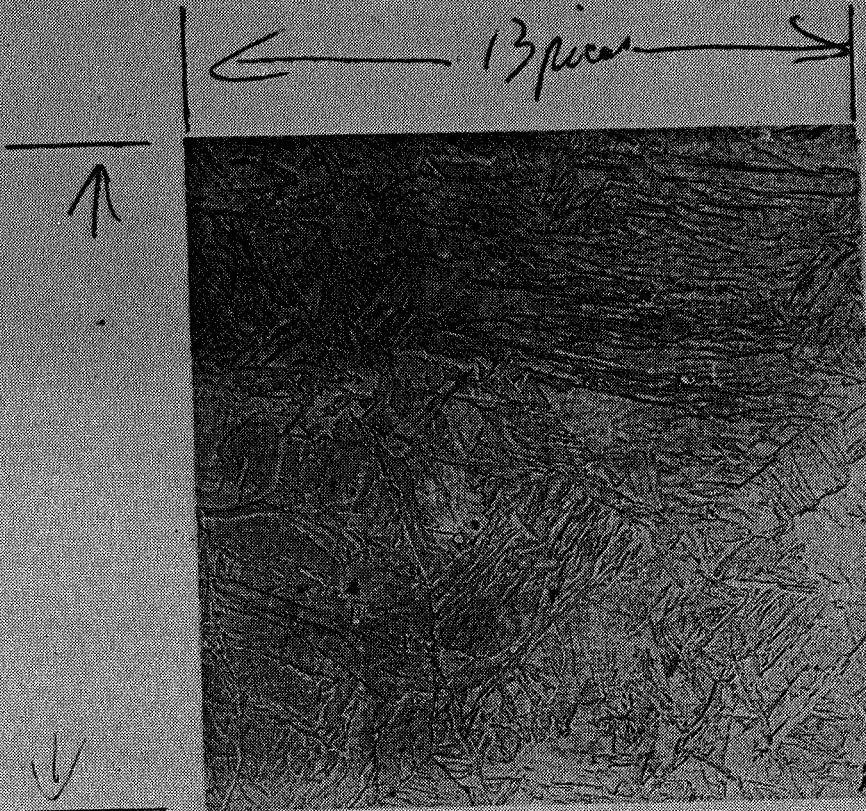


Figure 5

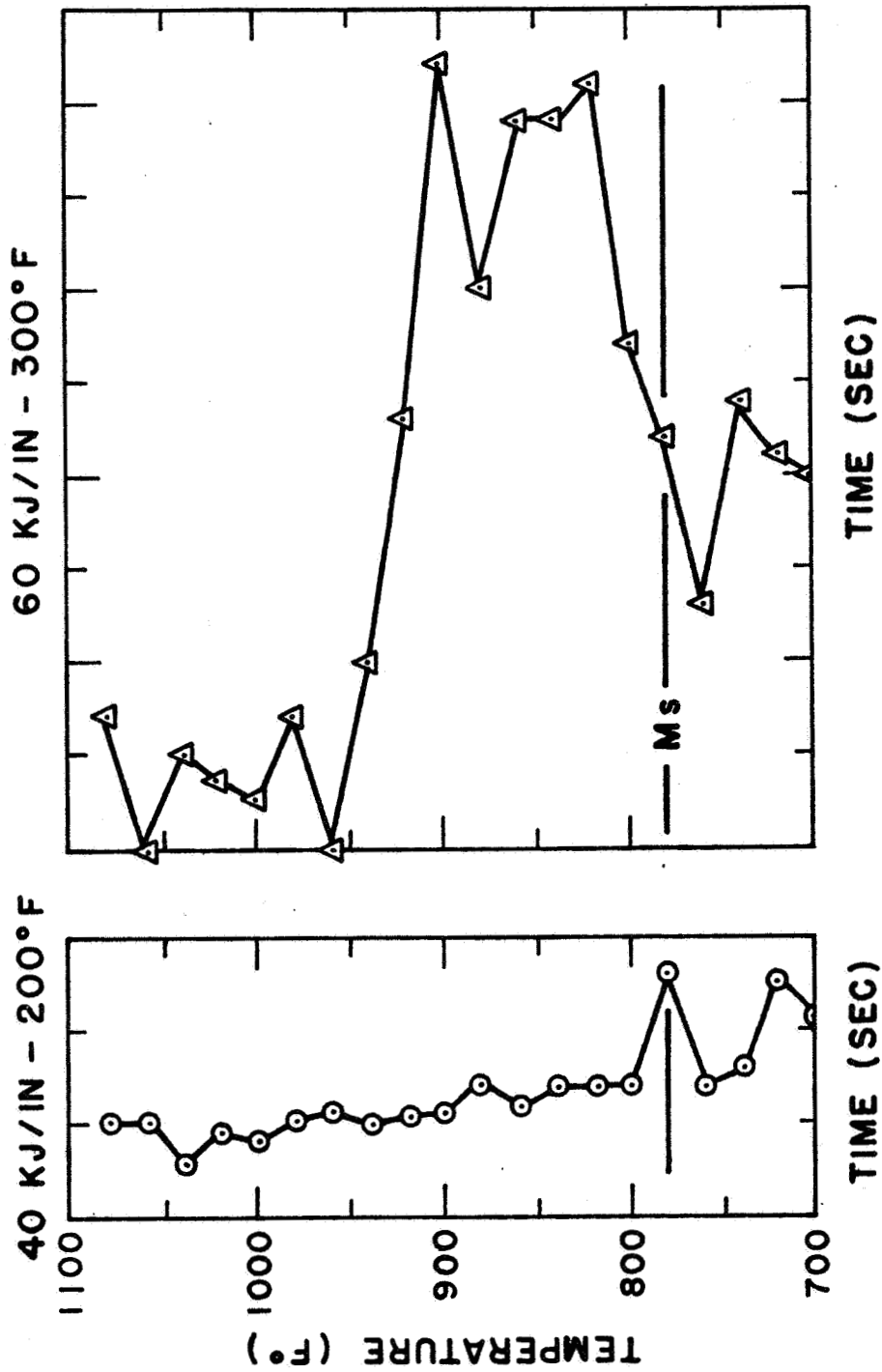
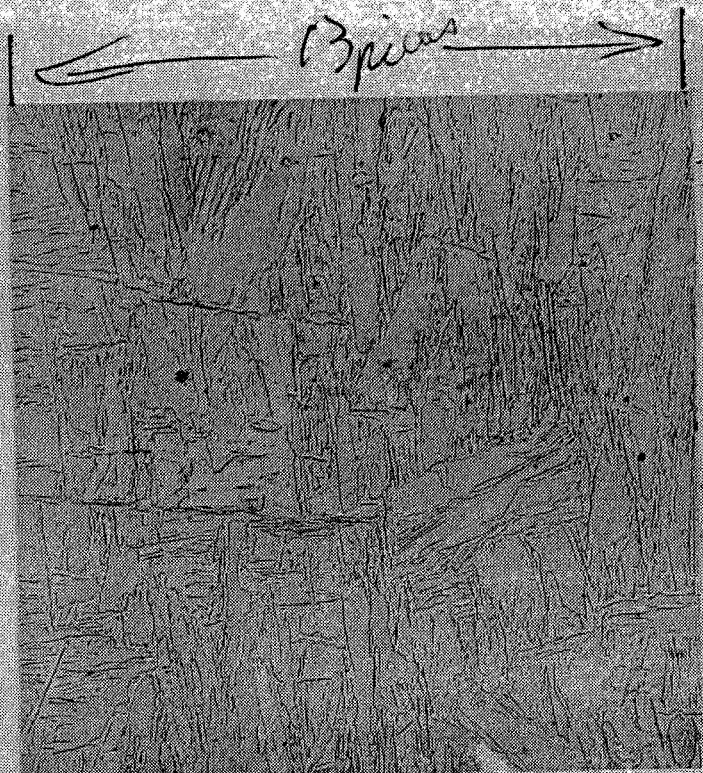


Fig. 6. INVERSE COOLING RATE ANALYSIS OF 1900°F AUSTENITIZATION WELD THERMAL CYCLES OCCURRING AT 40 KJ/IN.-200°F AND 60 KJ/IN.-300°F WELDING CONDITIONS.

↑



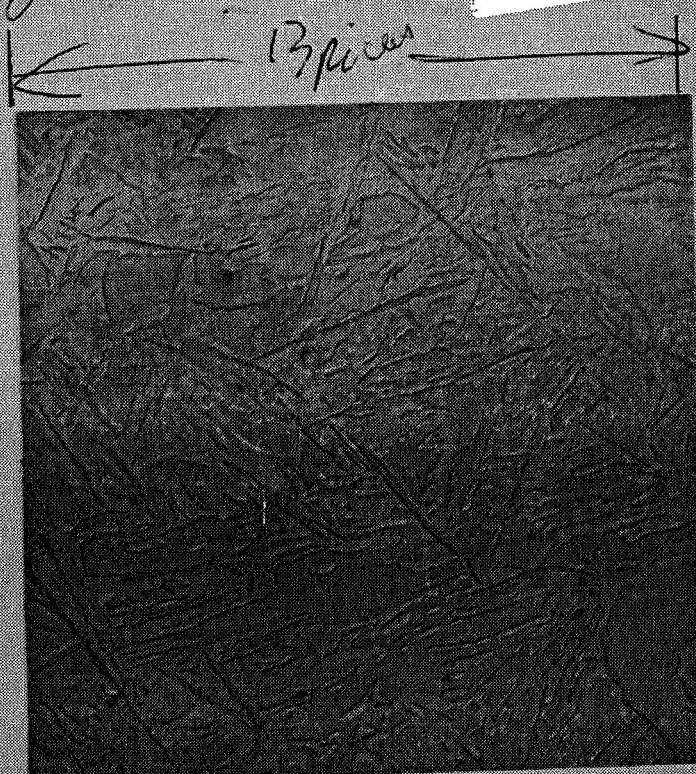
62.6

↓

Figure 7A

Fig 7A - Kentucky

↑



63.7

↓

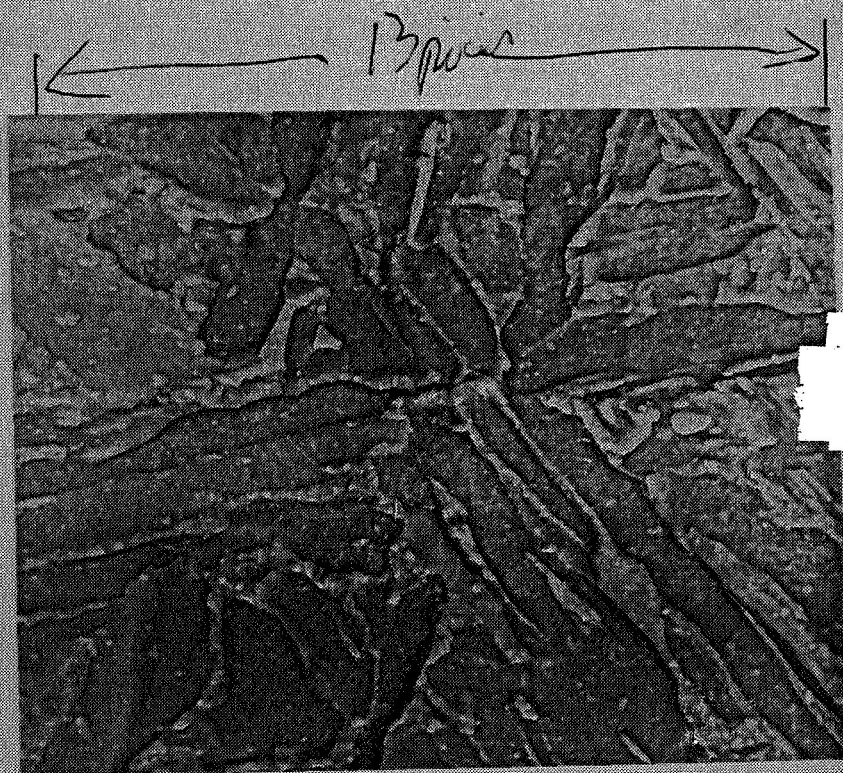
Figure 7B



53.0

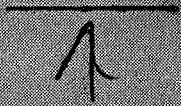
Figure 8A

Fig 8A - K sand



53.0

Figure 8B



← 13 pieces →

65.1
~~65.1~~

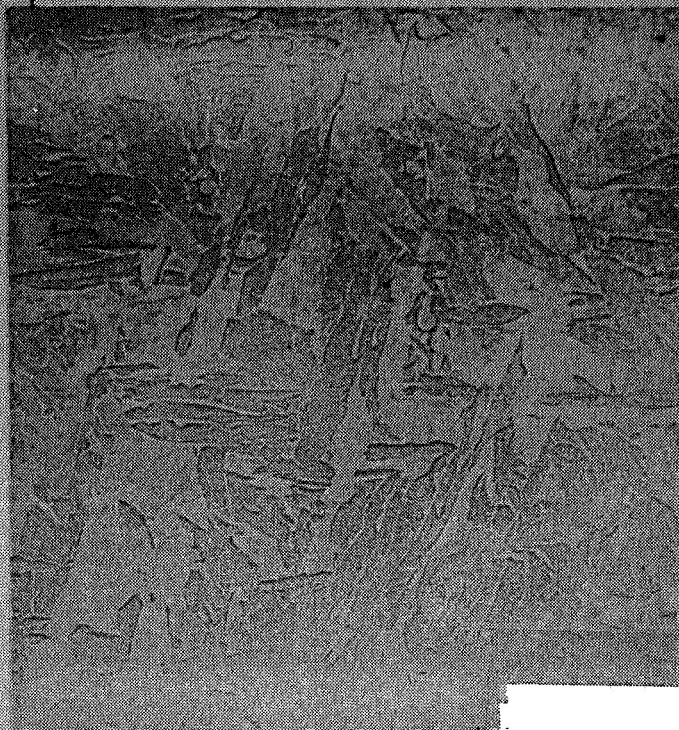
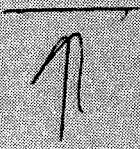


Figure 9A

Fig 9A - Krentz

← 13 pieces →

66.3



496<

Figure 9B

67.5

← 13 mic →

↑



↓

Figure 10A

Fig 10A - Kwanty

← 13 mic →

↑



67.5

↓

Figure 10B

497<

637

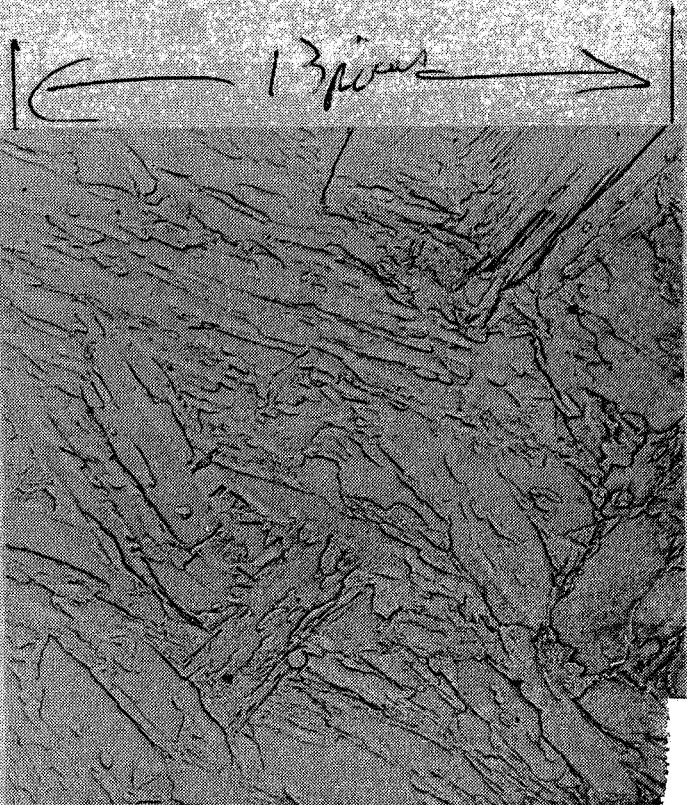


Figure 11A

Fig 11A - K. rauty

637



Figure 11B

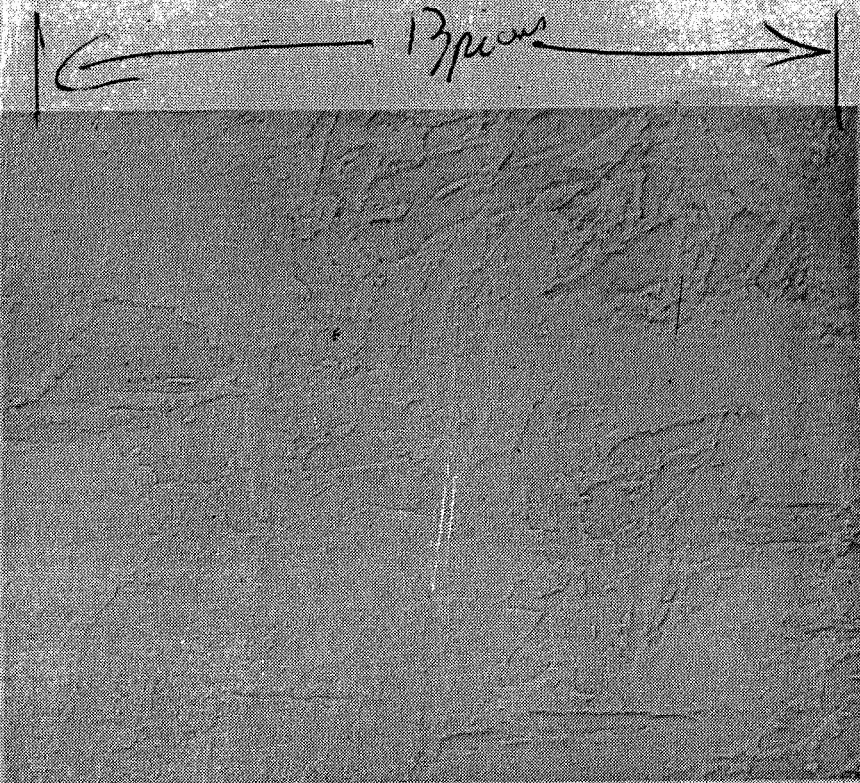


Figure 12A

Fig 12A - 600x

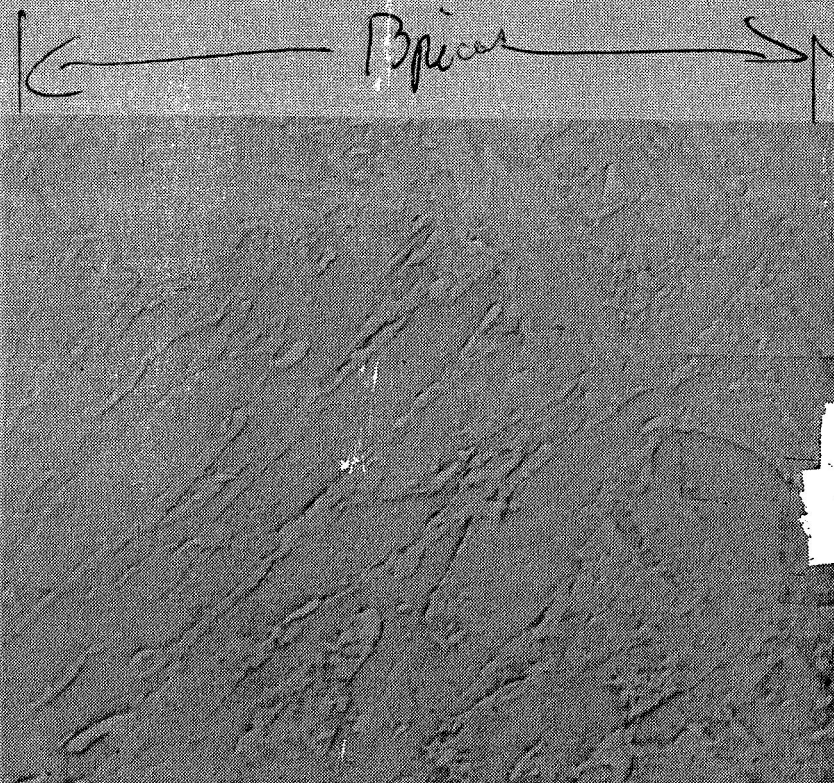


Figure 12B